

Roger Williams University

DOCS@RWU

Architecture, Art, and Historic Preservation
Faculty Publications

Architecture, Art, and Historic Preservation

8-1-2020

CREASE: Synchronous gait by minimizing actuation through folded geometry

Olga Mesa

Saurabh Mhatre

Dan Aukes

Follow this and additional works at: https://docs.rwu.edu/saahp_fp



Part of the [Architectural Engineering Commons](#), and the [Architectural Technology Commons](#)

CREASE: Synchronous gait by minimizing actuation through folded geometry

International Journal of
Architectural Computing
2020, Vol. 18(4) 385–403
© The Author(s) 2020
Article reuse guidelines:
sagepub.com/journals-permissions
DOI: 10.1177/1478077120948204
journals.sagepub.com/home/jac



Olga Mesa^{1,2}, Saurabh Mhatre¹  and Dan Aukes³

Abstract

The Age of the Fourth Industrial Revolution promises the integration and synergy of disciplines to arrive at meaningful and comprehensive solutions. As computation and fabrication methods become pervasive, they present platforms for communication. Value exists in diverse disciplines bringing their approach to a common conversation, proposing demands, and potentials in response to entrenched challenges. Robotics has expanded recently as computational analysis, and digital fabrication methods are more accurate and reliable. Advances in functional microelectromechanical components have resulted in the design of new robots presenting alternatives to traditional ambulatory robots. However, most examples are the result of intense computational analysis necessitating engineering expertise and specialized manufacturing. Accessible fabrication methods like laminate techniques propose alternatives to new robot morphologies. However, most examples remain overly actuated without harnessing the full potential of folds for locomotion. Our research explores the connection between origami structures and kinematics for the generation of an ambulatory robot presenting efficient, controlled, and graceful gait with minimal use of components. Our robot ‘Crease’ achieves complex gait by harnessing kinematic origami chains rather than relying on motors. Minimal actuation activates the folds to produce variations in walk and direction. Integrating a physical iterative process with computational analysis, several prototypes were generated at different scales, including untethered ones with sensing and steering that could map their environment. Furthering the dialogue between disciplines, this research contributes not only to the field of robotics but also architectural design, where efficiency, adjustability, and ease of fabrication are critical in designing kinetic elements.

Keywords

Digital fabrication, robotics, origami, laminate construction, smart geometry, digital manufacturing and materials, smart materials

¹Harvard University, Cambridge, MA, USA

²Roger Williams University, Bristol, RI, USA

³Arizona State University, Mesa, AZ, USA

Corresponding author:

Saurabh Mhatre, Harvard University, 48 Quincy Street, Gund Hall, Cambridge, MA 02138-3000, USA.

Email: smhatre@gsd.harvard.edu

Introduction

Advances in computational analysis and CAD/CAM fabrication methods have contributed greatly to the development of robotics. Regarding ambulatory robots, legged robots have been designed to fulfill specific functions and access tough terrain. Expertise in robotics is necessary to produce these types of robots. Iteration is usually slow, costly, and reserved for engineering disciplines. Innovations in the production of electromechanical components from the meter to the millimeter-scale have expanded the scale at which functional ambulatory robots are produced,^{1,2} but these examples remain accessible only to specialized fields.

Based on these limitations other fabrication methods have emerged as options for producing non-traditional robots. Research on origami-inspired designs³ and lamination techniques have produced functional designs that are more economical and faster to produce.⁴ However, in the majority of these cases, overly actuated designs remain a challenge.

Within the context of the fourth Industrial Revolution, where design and engineering disciplines are more integrated, questions about how they inform each other emerge. Can principles of origami paired with architectural design thinking help to overcome some of the challenges associated with traditional approaches to robotic engineering? What concepts that emerged from robotic design translate into opportunities in architectural design and applications?

The literature review shows opportunities to expand existing work on robotics, which established the following research goals for our investigation:

- Engage in an integrated approach involving design and engineering by proposing an unconventional robotic design approach.
- Use principles of origami in connection to kinematics to create an under-actuated ambulatory robot that features a complex gait.
- Expand the access of robotic design and deployment to a wider audience by employing a simple method of fabrication.
- Establish connections between this research and architectural design by exploring possible translations and scalability for architectural applications.

This research builds upon principles of action origami.⁵ Rather than adding unnecessary electromechanical actuators, the research relates folded geometry to kinematics, thereby offering efficient and easy-to-build robots with complex gait. The design, fabrication methods, and sensing capabilities identified in this research potentially contribute to the design of kinetic architectural components and surveying of architectural sites.

Background

While traditional, rigid robots dominate industrial robotics due to their stiffness, repeatability, and precision, their lack of adaptability in less structured contexts has the potential to harm robot, user, and the environment. Thus, in recent years, research has shifted toward using softer materials in the design, especially for those robots interacting with humans.⁶ The integration of compliant materials like rubber, fabric, etc., within jointed kinematic systems, can create a mechanical “fuse” that separate high-power actuation from the end-effectors and mimic soft interactions often found in the natural world.⁷

Origami-inspired robots originated in early MEMS research, wherein planar processes—layered, additive, etching, and optical lithography—were used to realize silicon-based hinges capable of rotating out of plane.⁸ Further research investigated larger flexure-based hinges to permit small-radius bending, relying on the mechanics of thin, compliant materials for rotary motion instead of interference-based mechanical pin joints.⁹ Additional work over the years has demonstrated the integration of

springs¹⁰ and considered the effect of material damping,¹¹ the essential elements of dynamic systems. Unlike common mechanical elements found in more traditional robotic systems, these components are constructed using planar fabrication techniques in which compatible materials are iteratively added and removed to create a monolithic, multi-material, electro-mechanical system. These concepts have been demonstrated at nano, micro, millimeter, and centimeter scales, in materials as disparate as silicon,⁸ carbon fiber,¹² titanium,¹³ plastic, and cardboard.¹⁴ These technologies promise to solve novel problems, either at size scales where traditional mechanical devices such as gears, bearings, and motors are unavailable or at cost-scales which envision industrial-scale processes fabricating large numbers of inexpensive robots.^{15–17}

Softer materials also shift the focus during the design of robotic systems from a position-controlled to a force-dependent domain, where joint compliance and under actuation—a lower number of actuators than degrees of freedom in a system—plays a critical role in determining the static configuration of kinematic systems in equilibrium.¹⁸ Thus, the role of material properties and geometry in compliant flexure joints can significantly alter the motion of a robotic system, especially given external interactions with the world.^{19,20} In the case of legged robots, such interactions come in the form of ground reaction forces. Though in free space an underactuated robot may exhibit a single prescribed path as its actuators move it around, the presence of external ground reaction forces in an underactuated systems plays a significant role in changing the gait and performance of robots walking on the ground in the presence of gravity.

Legged locomotion has been a focus of robotics research for decades.^{21,22} Legged systems are often touted for their ability to negotiate varied terrain and step over obstacles,²³ as well as to move in human environments in a more human way.²⁴ A variety of topics have been studied in the context of legged locomotion, including the role stiffness plays in actuators,²⁵ feet,²⁶ spines,²⁷ and legs.²⁸ Legged systems, however, are often quite expensive, limiting access to and research on these systems.

Some bio-inspired ambulatory robots show that folding mechanisms are a scalable and cost-effective technique to achieve actions such as walking,²⁹ running,^{14,30,31} jumping,^{31,32} and flying. Several research groups have proposed strategies for actuating and powering foldable devices.^{33–36} In recent decades, advances have been made in how to design,^{4,34} manufacture,³⁷ and analyze origami-inspired hinged designs. Using FEA, methods have been developed³⁸ to analyze the dynamics of these robots,^{11,39} to identify functions and integrate modular components.⁴⁰

Even with the shift towards laminate fabrication, researchers rarely examine the role under-actuation can play in simplifying control needs.⁴¹ Under-actuation can be considered a tool for shifting computational complexity from the time of use—wherein high-speed controllers set actuator outputs at each joint in real-time based on the state of the system and the desired output—to design time, wherein designers must anticipate use-cases and design systems that respond with good performance throughout a variety of different external stimuli.¹⁹ The potential for under-actuation to permit a variety of responses, as well as to reduce complexity and cost, may be thought of as potential benefits in architectural cases as well.

Robotics and kinetic architectural design share similar needs of achieving components that display elegant movement, are lightweight, robust, easy to manufacture, durable, and efficient. Thus, solutions for one might translate to the other.

Origami has been used for generating effective three-dimensional forms from flat sheets. On-going research has proved that scaling-up origami concepts to Architecture and beyond is possible.^{42–44} Thick-origami methods by Tachi and others show promise in successfully translating origami from the millimeter to the meter-scale.^{45–47} However, most applications in architecture have focused on static states⁴⁸ that overlook the dynamic phases of these systems. Some examples have successfully translated origami principles to kinetic facades and installations^{49,50} like in the case of Hoberman and Associates' work^{51–53} and Aedas Architects.⁵⁴ However, these examples often rely on complicated actuation systems requiring numerous mechanical parts.

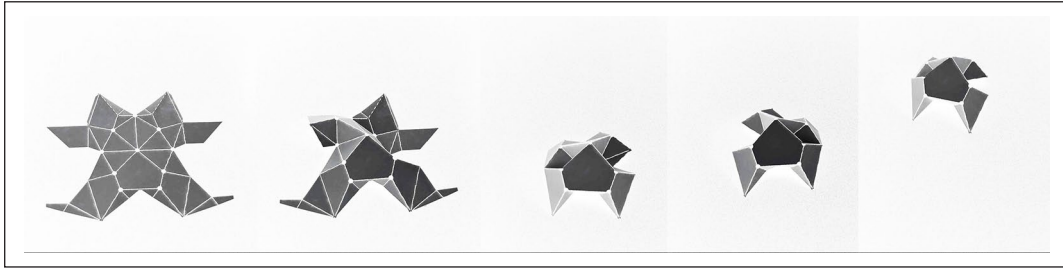


Figure 1. Transformation from two to three-dimensional configurations. (Adapted from publication).³⁴

Methods and results

The research integrated digital and physical workflows that involved testing prototypes at different scales. The relationship between the folded pattern and kinematics was studied through physical iterations and actuated in different ways. The successful patterns were digitally modeled and refined based on digital simulations. Then, prototypes were fabricated rapidly using a laminated technique. Various materials for the rigid planes and the flexible joints were explored, as well as the type, number, and position of the actuators. The prototypes were programmed to achieve gait control, steering, and navigation.

Relationship between folded pattern and kinematics

Crease features a series of rigid planes connected by flexible joints. Being a robot generated by origami principles, *Crease's* three-dimensional configuration results in a developable pattern when flat (Figure 1). The relationship between the folded pattern and movement was studied through an iterative process of physical and digital design. The pattern was inspired by observing how the human body's upper extremities move as the torso rotates. Applying principles of parallel and spherical linkages to folded geometry, the origami waterbomb base (Figure 2(a)), a spherical linkage commonly used in origami structures,⁵⁵ was employed to allow rotational mobility of the upper body. It was then modified by removing one of its folds to create a grounding base for the actuation element (Figure 2(b)).

Crease's two-dimensional mountain-valley pattern shows symmetry along the *y-axis*. The modified waterbomb base connects to the folds that make the robot's legs: two rear and two front legs (Figure 3). These act as parallel linkages that allow repetitive motion. Although the rigid planes are connected with flexible joints, in their three-dimensional configuration, various elements that fulfill a particular role can be identified such as the leg connector, the front body, etc. (Figure 3).

The locomotion of *Crease* is accomplished by utilizing rotational motion to activate the interconnected folds that make up its body.³⁴ Actuation element/s is/are placed on the inner rear part of the body to actuate the origami pattern. The design and flexibility of the folds allow the force of the motor to circulate throughout the body. Rotational action creates a corresponding and synchronized movement of the legs. As the rear and front legs of one side unfold, the legs of the other side fold. Figure 4 shows the gait cycle starting with a neutral position (*Position A*). As the torso rotates, the distance between points *P3* and *P4* increases while it decreases between points *P1* and *P2* making the left leg move forward (*Position B*). The left front leg raises higher than the other three as this happens. Afterward, the robot returns to *Position A* and as the distance between points *P1* and *P2* increases and decreases between points *P3* and *P4*, the right leg moves forward (*Position C*). The gait cycle starts again as torso rotation occurs (Figures 4–7).

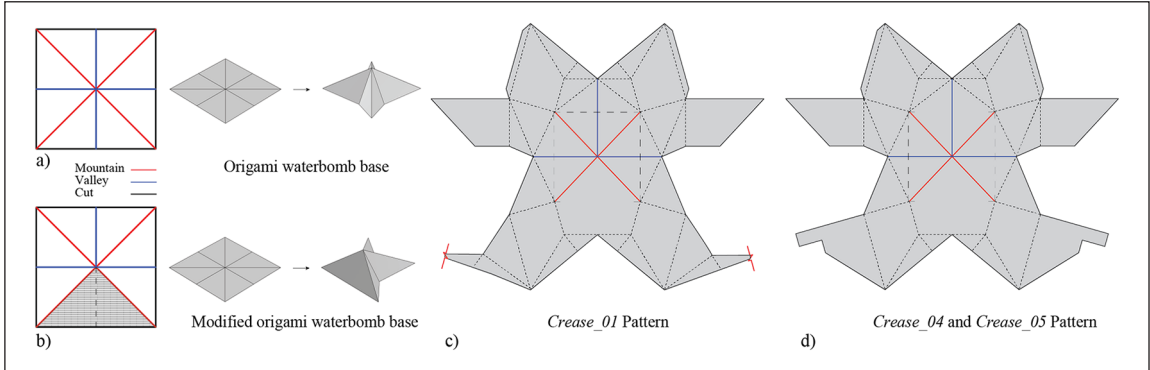


Figure 2. (a) Origami waterbomb base (b) Modified waterbomb, and (c) Crease's folding pattern showing modified waterbomb. (Adapted from publication).³⁴

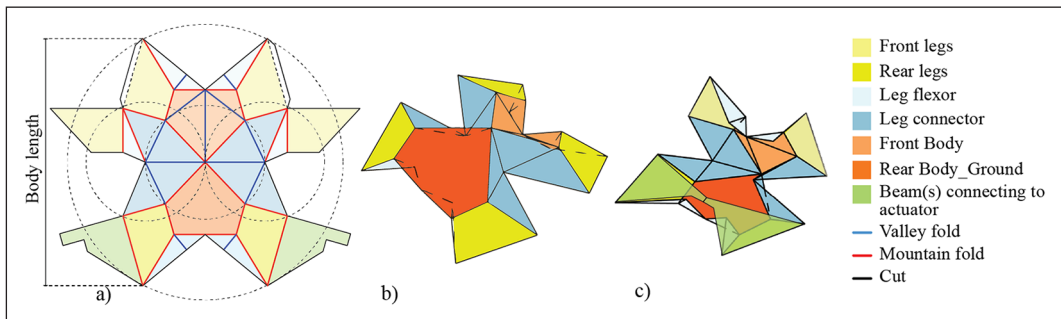


Figure 3. (a) Crease folding pattern with identification of the roles (b) 3D top view, and (c) 3D Underside view. (Adapted from publication).³⁴

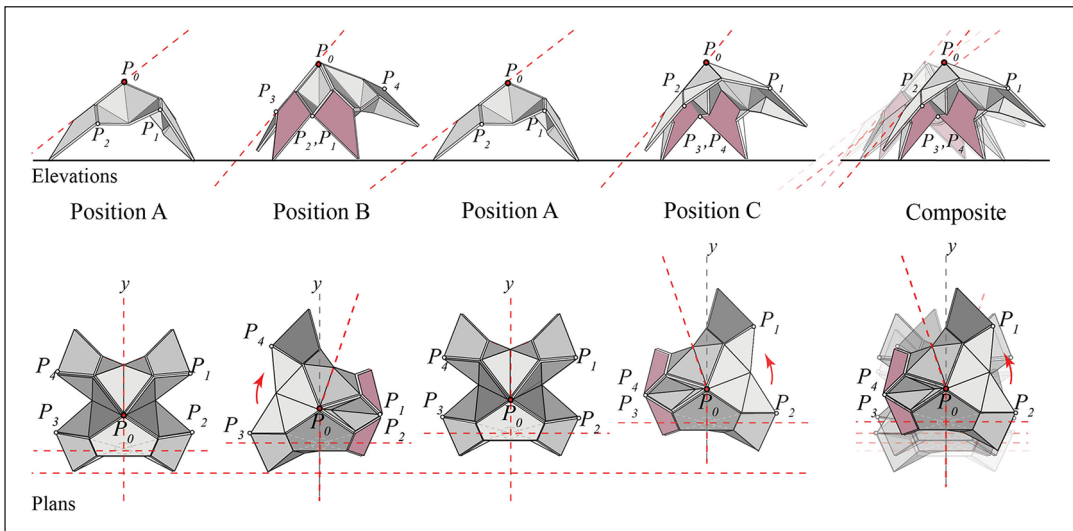


Figure 4. Cycle showing Crease's gait. Adapted from publication).³⁴

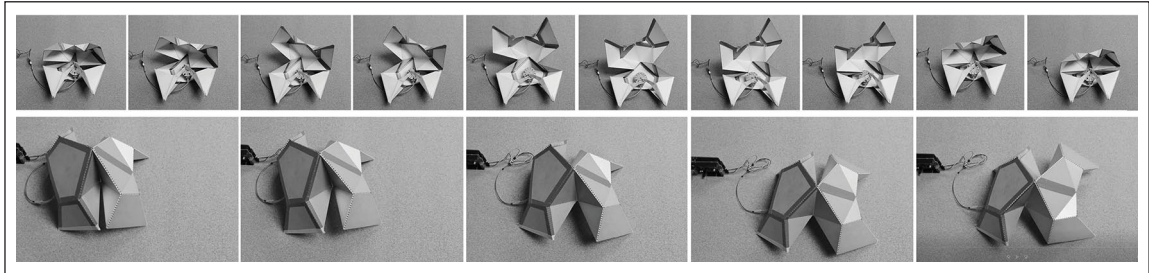


Figure 5. Crease_01 Step sequence.

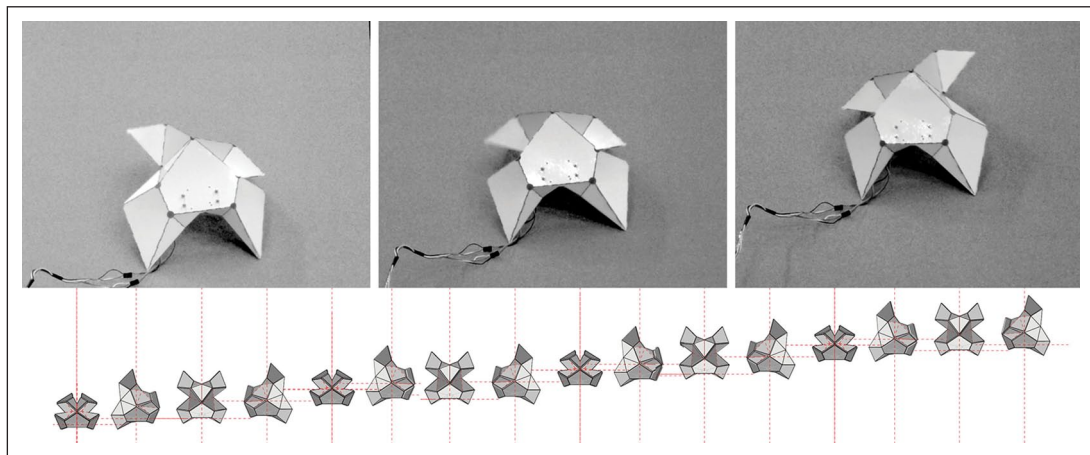


Figure 6. Crease_04 Step sequence.

Iterations

The proportions of the folded pattern in relation to gait were studied both physically (Figure 8) and digitally (Figure 9). After exploring variations without a front rib, different dimensions for waist and front and hind legs, the selected pattern (shown in Figure 3) was chosen, as it presented a balance between stability and controlled movement. The size, actuation, range of motorized rotation, and navigation control were all variables taken into account to produce iterations of the origami robot. In terms of size, prototypes from 6 to 45 cm in body length were generated (Figure 3). For actuation, stepper motors or servomotors were used in the 20–45 cm prototypes to understand the different possibilities offered by each type. The number of motors and their location relative to the origami body were documented. Regarding navigation, both tethered and untethered origami robots were produced (Table 1). In these variations, significant differences in gait and navigation control were observed. These are exemplified by the following prototypes: *Crease_01*, *Crease_04*, and *Crease_05* (Figure 8) and described below in the following sections. 3.3, 3.3.1, 3.3.2, and 3.4.

Programming

Tethered and un-tethered versions of *Creases* ranging from 20 to 45 cm in body length were manufactured. In the tethered versions, a single stepper motor was attached to the ground plane and controlled by

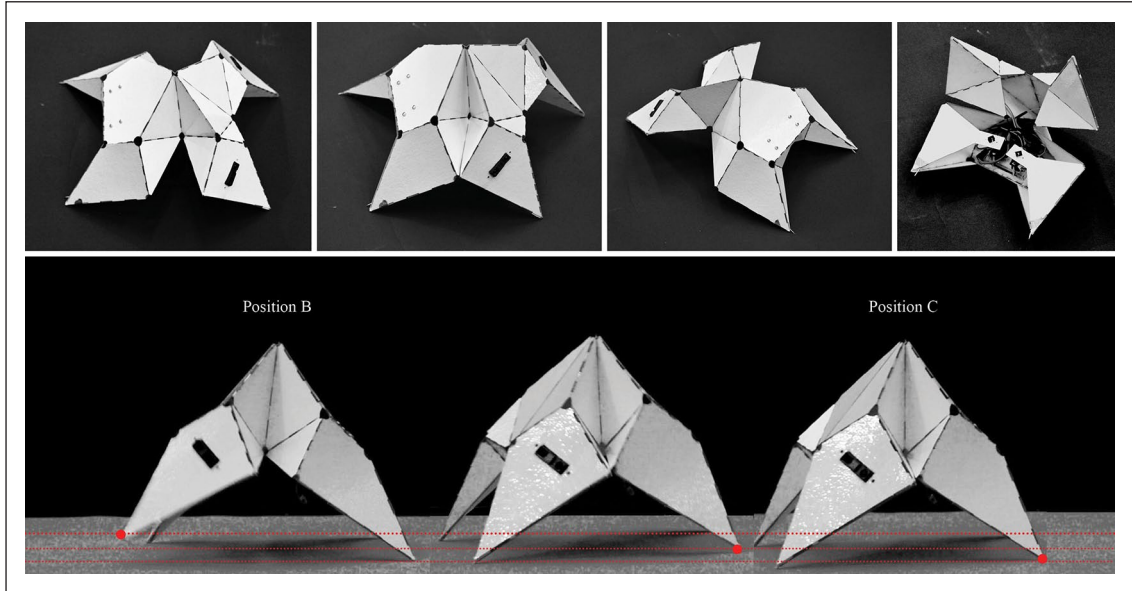


Figure 7. Untethered Crease_05 gait cycle. (Adapted from publication).³⁴

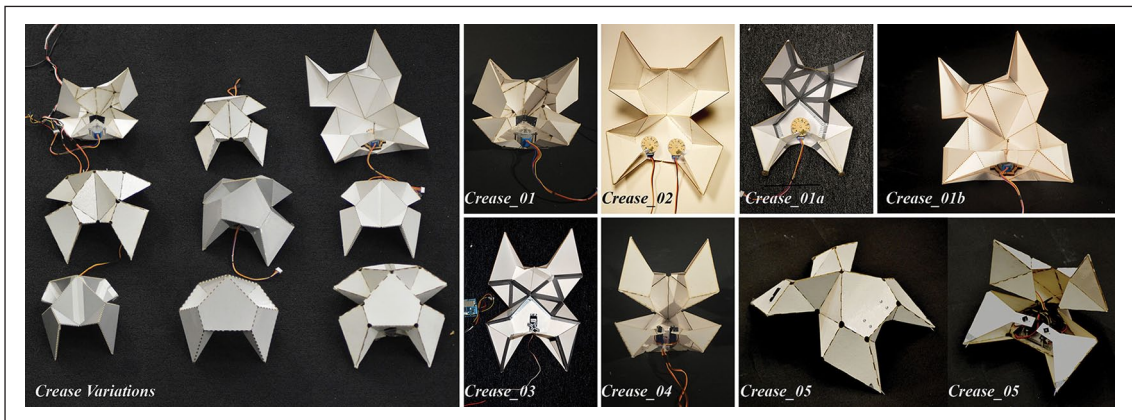


Figure 8. Selected prototypes. (Adapted from publication).³⁴

an *Arduino Uno* via an *Adafruit Motor shield v2.3*. To keep the whole assembly lightweight in the untethered versions, a light *Arduino Nano* and a *Lithium-ion* battery controlled the two servo motors connected to the base.

Actuation. *Crease_01* and *Crease_04* both have the same pattern only differentiated by the way their legs connect (Figure 2) to the actuation element and the type of actuators used. Figure 10 shows the legs of *Crease_01* attached to one folded beam where point $P5$ is at junctions between axis x and y $(0, 0)$. In *Positions A*, *Crease_01* is in a neutral position (Figures 4 and 10). The stepper motor controls the rotation of point

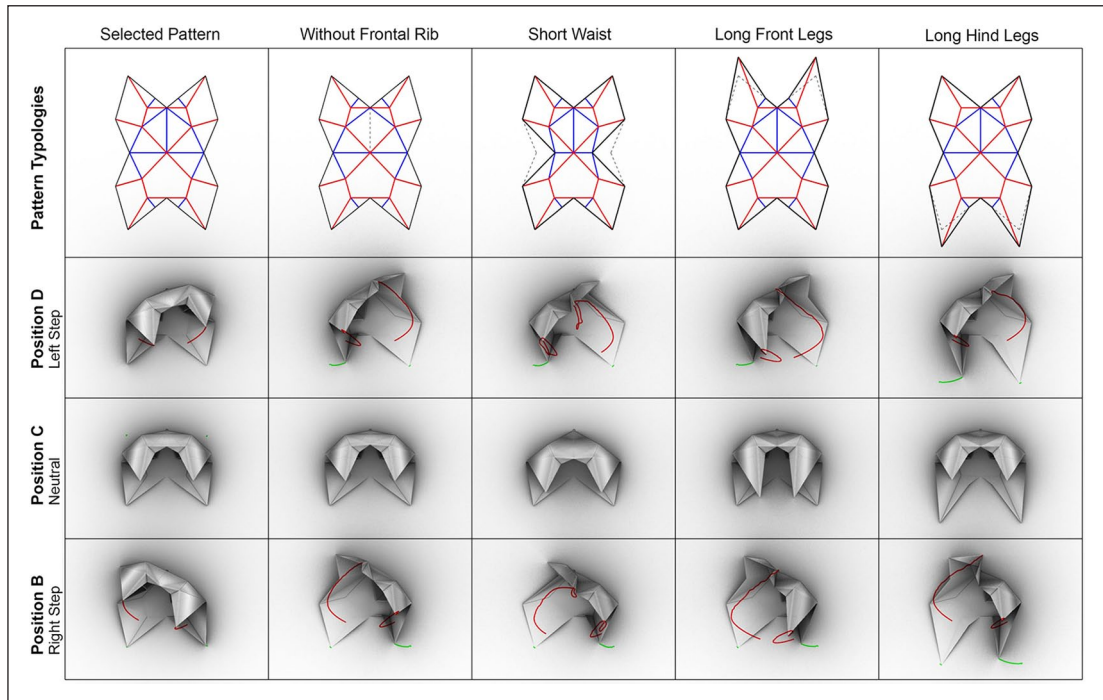


Figure 9. Study of input angles (green) and output angles (red) relative to the folding pattern using Kangaroo for Grasshopper.

Table I. Crease variations (adapted from publication).³⁴

Crease type	Folded beam	Stepper motor	Servo motor	Bluetooth control	IR sensor	Size
Crease_01	(1)	(1)	–	–	–	25 cm
Crease_02	(2)	(2)	–	–	–	25 cm
Crease_03	–	–	(1)	–	–	25 cm
Crease_04	–	–	(2)	–	–	25 cm
Crease_05	–	–	(2)	(2)	(2)	30 cm

$P5$ causing the legs to fold or unfold. Within a 360° cycle, $Crease_01$ moves in a straight gait, from $Position B$ to $Position C$ (Figure 10). When $P5$ is in the $(+x, +y)$ quadrant, the distance between points $P1$ and $P2$ decreases while the distance between points $P3$ and $P4$ increases (Figure 10(a)). Figure 10(c) shows that the opposite happens if $P5$ is in the $(-x, +y)$ quadrant.

Figure 11 shows the legs of $Crease_04$ paired up with a corresponding folded beam and servo motor. In a straight gait, $Crease_04$ moves from $position B$ to $position C$ every 180° cycle of each servomotor (Figure 11). If points $P8$ and $P9$ are in the $(+x, +y)$ quadrant, the distance between points $P1$ and $P2$ decreases while the distance between points $P3$ and $P4$ increases (Figure 11(a)). Figure 11(c) shows that the opposite happens when points $P8$ and $P9$ are located in the $(-x, +y)$ quadrant.

$Crease_01$ (Figure 5) presents a more fluid and slower walk than $Crease_04$ (Figure 6). By having one servomotor paired to a hind leg, $Crease_04$ has the ability to change the direction of its walk. $Crease_05$, as $Crease_04$, can steer but $Crease_05$ is untethered (Figure 7).

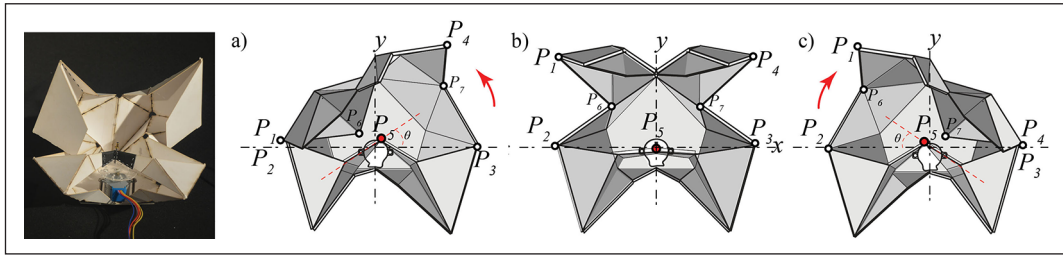


Figure 10. Underside view of Crease_01. (a) Position B (b) Position A, and (c) Position C. (Adapted from publication).³⁴

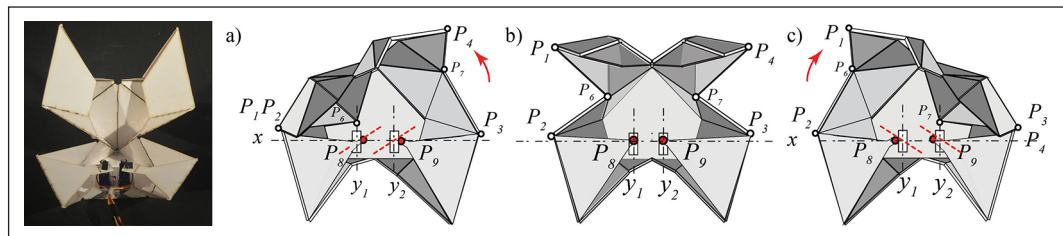


Figure 11. Underside view of Crease_04. (a) Position B (b) Position A, and (c) Position C. (Adapted from publication).³⁴

Steering and sensing. *Crease_04* and *Crease_05* achieved a high degree of control and ability to steer in different directions. These prototypes displayed straight walk, soft and sharp turns as well as and 360° turns. This was accomplished by pairing a rear leg to a corresponding servo motor. For a straight walk, both servos start from their neutral *Position A* (90°) and then oscillate synchronously between 0° to 180° (from *Position B* to *C*) (Figure 12(a)). For turning in a particular direction, one servo's range of motion is reduced relative to the other (Figure 12(b)). This causes one leg to act as a pivot and the other leg to guide direction (Figure 12(b) and Figure 13). For example, right turns were achieved by reducing the angle domain of the servomotor #2 (which controls the hind left leg) in relation to servomotor #1. For sharper turns, the angle domain was further reduced with respect to the other as seen as an example in the *Sharp Right* case in Figure 14. Therefore, the greater range of motion of the left leg steered the robot to the right (Figure 12(b)) and vice versa. The angle domains are shown in Table 2. It is also possible for the robot to make a U-turn and reverse its path (Figure 13).

Figure 14 shows different cases with gait directions. Each the rotation of the servomotor #1 (red line) and the servomotor #2 (dotted blue line) is recorded in relative to time. Servomotor #1 is connected to the left hind leg and servomotor #2 is connected to the right hind leg. In all the charts, both servos start from their neutral position (90°). For example, in the *Straight Gait*, the angles recorded for both servos are 90°, 0°, 90°, 180°, 90° whereas for the *Slight Right Gait* the angles recorded for servomotor #2 are: 90°, 0°, 90°, 0°, 90°.

In *Crease_04* (tethered), the input cases of the code were provided manually with potentiometers connected to an *Arduino*. This formed an open-loop system. In *Crease_05*, the code formed a closed-loop system using automatic inputs from a pair of infrared sensors connected to the front legs that in-turn controlled the servos (Figure 15). This established a real-time feedback loop that allowed *Crease_05* to avoid obstacles while walking (Figure 13). The infrared sensors measured the distance to any approaching obstacles and assigned it to a case in the code. If there were no obstacles, the robot would walk straight. If an obstacle were far the robot would make a soft turn, and if it were close, it would make a sharp turn (Figure 13). *Crease_04* and *Crease_05* can make full turns as shown in case 6 in Figure 13.

A simple *Arduino* code was used to control the stepper motor and the servos in the various *Crease* iterations (Figure 16). The code controlled the rotational domains of the actuators and was divided into the

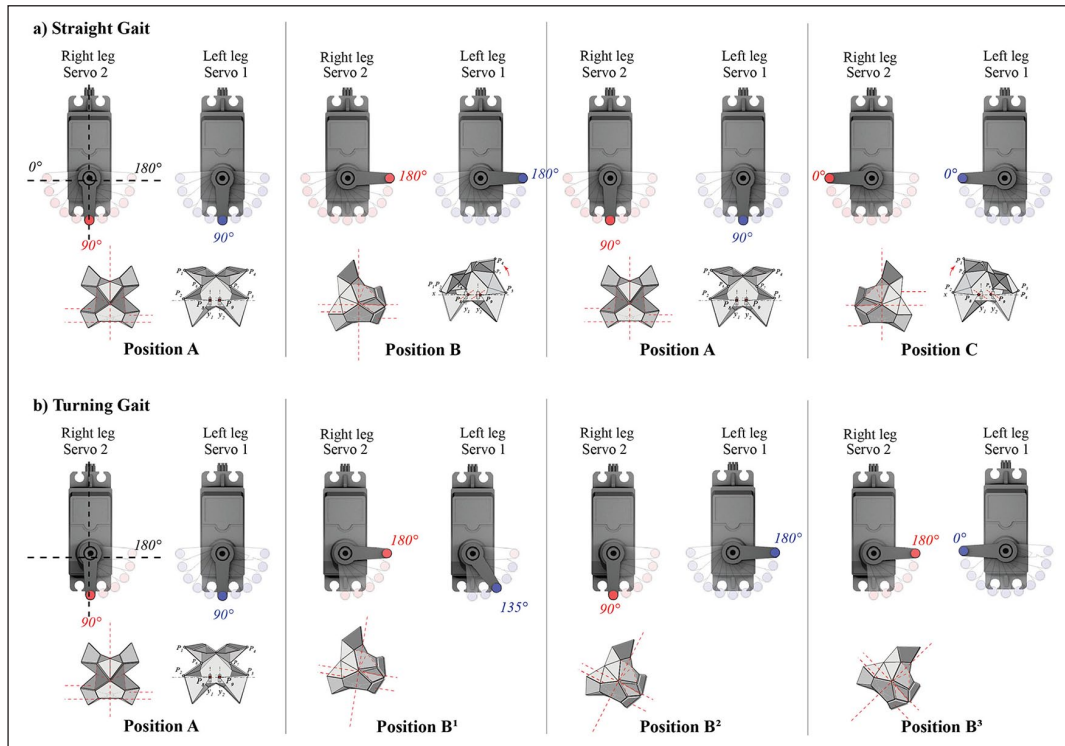


Figure 12. Servomotor positions as seen from the underside of Crease_04. (a) Straight gait (b) Turning Gait. (Adapted from publication).³⁴

following cases: *straight*, *stop*, *hard left*, *soft left*, *hard right*, and *soft right*. Some details of the code are highlighted below.

The location of the obstacles is sensed by the two infrared sensors, *IR1* and *IR2* respectively, and their values are assigned to the cases mentioned above. The function ‘servo_move’ cycles between the rotational domains of the assigned cases and then it sends the values to the respective servo.

Digital analysis

The multiple degrees of freedom and the underactuated nature of the mechanism makes *Crease's* gait very challenging to simulate by traditional means. The following workflow simply confirms a few of the possibilities of the kinematics of its motion.

Analysis of the translation from a flat sheet to its three-dimensional configuration was possible using Origamizer⁵⁶ and Origami Simulator.⁵⁷ Both these softwares are easy to use and have a simple user interface which made it possible to rapidly test multiple pattern iterations and simulate their respective folded 3D configurations. Origami Simulator also aided in finding planar relationships between the rigid planes through one of its normal mapping features (Figure 17(a)). The kinematic chain formed between the faces of the hind legs and front legs was studied using Dassault Solidworks, McNeel Rhino, Grasshopper, and Kangaroo⁵⁸ workflows. Within these softwares, the monolithic origami laminate could be discretized into a series of rigid planes and dynamic hinge joints showing similar kinematics. This enabled analyzing the co-relationship between the folding angles of the hind legs and the impact they have on the longitudinal

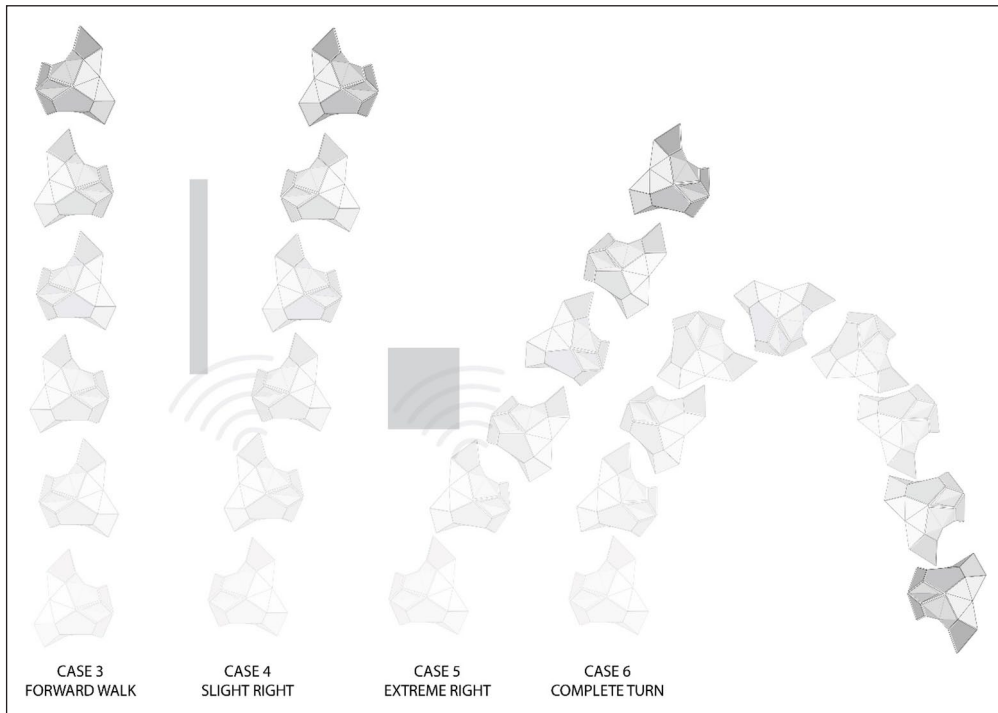


Figure 13. Sensing and steering case studies.

and latitudinal displacement on the front legs. Figure 9 shows pattern iterations and the corresponding resultant motions.

Manufacturing technique

Crease prototypes were fabricated using a pop-up laminate construction where the flexible material was adhered in between two rigid planes. This method was fast and economical enabling the efficient production of several iterations. A *Universal 150W* laser cutter was used to cut the pattern of rigid planes, removing material away for the flexible membrane to form the folds. Adhesive layers were also laser cut to bond the flexible membrane to the rigid stock. Various flat materials were employed according to the size of the prototype.

A flexible 0.7 mm PET membrane adhered between two rigid planes of 3 mm *Bristol* card stock was used for the 20–45 cm prototypes (Figure 18). Circular perforations were used to relieve joint stress and registration marks ensured a precise assembly of the layers to be laminated. An *Apache AL18P* thermal laminator was used to bond the flexible material to the rigid stock through the adhesive layers.

Designed for model laminate constructions, *PopupCAD*,⁴ an open-source software, was employed to produce several laminated prototypes. Through this platform, the folds were optimized by using castellated and laminated hinges (Figure 18(b)). Weakened by castellation, the PET layer acted as a hinge with enough rigidity for the desired motion. The spacing and length of the cuts in the castellated hinges were tested to achieve the desired flexure. Figure 18(b) shows sections of the laminated layers to achieve a mountain or a valley fold.

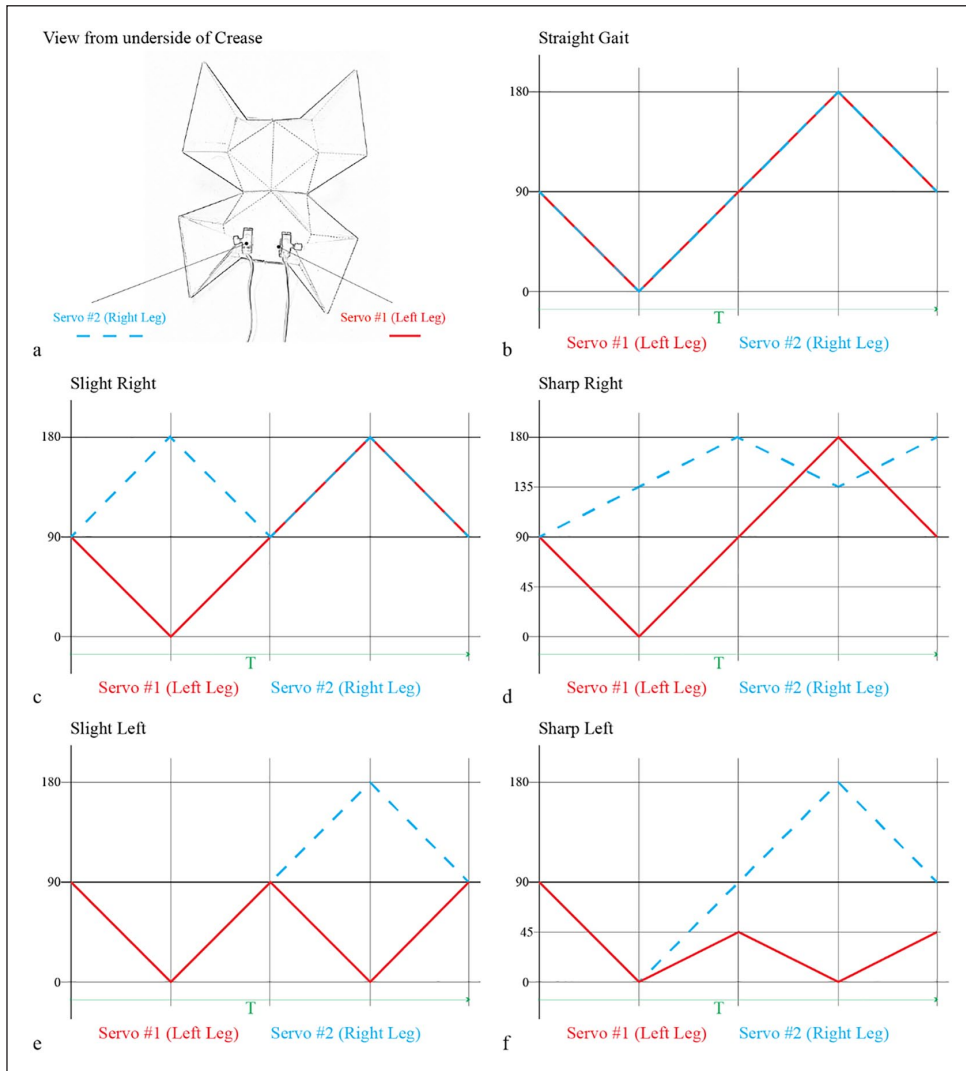


Figure 14. Gait directions relative to servo angle domains.

Table 2. Table showing servo angle domains of the two legs in relation to different gaits.

Gait	Right Leg (Servo #2)		Left Leg (Servo #1)	
	Start	End	Start	End
Sharp Left	0°	180°	0°	45°
Slight Left	0°	180°	0°	90°
Straight	0°	180°	0°	180°
Slight Right	90°	180°	0°	180°
Sharp Right	135°	180°	0°	180°
Stop	90°	90°	90°	90°

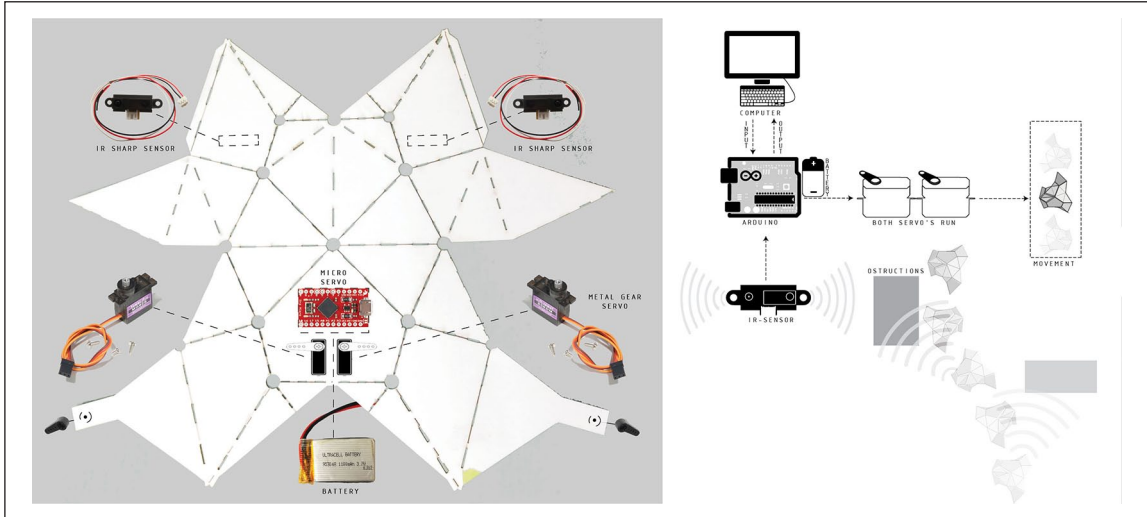


Figure 15. Crease_05 Actuation and sensing components. (Adapted from publication).³⁴

<pre> 39 void loop() 40 { 41 // READ SENSOR VALUES 42 I1_val = analogRead(I1); 43 I2_val = analogRead(I2); 44 map = sum(I1_val, I2_val); 45 // map average of values to 'Cases' 46 case = map(I1_val, 0, 1023, 1, 5); 47 case = map(I2_val, 0, 1023, 1, 5); 48 } 49 50 51 52 53 54 55 56 57 58 59 60 61 62 63 64 65 66 67 68 69 70 71 72 73 74 75 76 77 78 79 80 81 82 83 84 85 86 87 88 89 90 91 92 93 94 95 96 97 98 99 100 101 102 103 104 105 106 107 108 109 110 111 112 113 114 115 116 117 118 119 120 121 122 123 124 125 126 127 128 129 130 131 132 133 134 135 136 137 138 139 140 141 142 143 144 145 146 147 148 149 150 151 152 153 154 155 156 157 158 159 160 161 162 163 164 165 166 167 168 169 170 171 172 173 174 175 176 177 178 179 180 181 182 183 184 185 186 187 188 189 190 191 192 193 194 195 196 197 198 199 200 201 202 203 204 205 206 207 208 209 210 211 212 213 214 215 216 217 218 219 220 221 222 223 224 225 226 227 228 229 230 231 232 233 234 235 236 237 238 239 240 241 242 243 244 245 246 247 248 249 250 251 252 253 254 255 256 257 258 259 260 261 262 263 264 265 266 267 268 269 270 271 272 273 274 275 276 277 278 279 280 281 282 283 284 285 286 287 288 289 290 291 292 293 294 295 296 297 298 299 300 301 302 303 304 305 306 307 308 309 310 311 312 313 314 315 316 317 318 319 320 321 322 323 324 325 326 327 328 329 330 331 332 333 334 335 336 337 338 339 340 341 342 343 344 345 346 347 348 349 350 351 352 353 354 355 356 357 358 359 360 361 362 363 364 365 366 367 368 369 370 371 372 373 374 375 376 377 378 379 380 381 382 383 384 385 386 387 388 389 390 391 392 393 394 395 396 397 398 399 400 401 402 403 404 405 406 407 408 409 410 411 412 413 414 415 416 417 418 419 420 421 422 423 424 425 426 427 428 429 430 431 432 433 434 435 436 437 438 439 440 441 442 443 444 445 446 447 448 449 450 451 452 453 454 455 456 457 458 459 460 461 462 463 464 465 466 467 468 469 470 471 472 473 474 475 476 477 478 479 480 481 482 483 484 485 486 487 488 489 490 491 492 493 494 495 496 497 498 499 500 501 502 503 504 505 506 507 508 509 510 511 512 513 514 515 516 517 518 519 520 521 522 523 524 525 526 527 528 529 530 531 532 533 534 535 536 537 538 539 540 541 542 543 544 545 546 547 548 549 550 551 552 553 554 555 556 557 558 559 560 561 562 563 564 565 566 567 568 569 570 571 572 573 574 575 576 577 578 579 580 581 582 583 584 585 586 587 588 589 590 591 592 593 594 595 596 597 598 599 600 601 602 603 604 605 606 607 608 609 610 611 612 613 614 615 616 617 618 619 620 621 622 623 624 625 626 627 628 629 630 631 632 633 634 635 636 637 638 639 640 641 642 643 644 645 646 647 648 649 650 651 652 653 654 655 656 657 658 659 660 661 662 663 664 665 666 667 668 669 670 671 672 673 674 675 676 677 678 679 680 681 682 683 684 685 686 687 688 689 690 691 692 693 694 695 696 697 698 699 700 701 702 703 704 705 706 707 708 709 710 711 712 713 714 715 716 717 718 719 720 721 722 723 724 725 726 727 728 729 730 731 732 733 734 735 736 737 738 739 740 741 742 743 744 745 746 747 748 749 750 751 752 753 754 755 756 757 758 759 760 761 762 763 764 765 766 767 768 769 770 771 772 773 774 775 776 777 778 779 780 781 782 783 784 785 786 787 788 789 790 791 792 793 794 795 796 797 798 799 800 801 802 803 804 805 806 807 808 809 810 811 812 813 814 815 816 817 818 819 820 821 822 823 824 825 826 827 828 829 830 831 832 833 834 835 836 837 838 839 840 841 842 843 844 845 846 847 848 849 850 851 852 853 854 855 856 857 858 859 860 861 862 863 864 865 866 867 868 869 870 871 872 873 874 875 876 877 878 879 880 881 882 883 884 885 886 887 888 889 890 891 892 893 894 895 896 897 898 899 900 901 902 903 904 905 906 907 908 909 910 911 912 913 914 915 916 917 918 919 920 921 922 923 924 925 926 927 928 929 930 931 932 933 934 935 936 937 938 939 940 941 942 943 944 945 946 947 948 949 950 951 952 953 954 955 956 957 958 959 960 961 962 963 964 965 966 967 968 969 970 971 972 973 974 975 976 977 978 979 980 981 982 983 984 985 986 987 988 989 990 991 992 993 994 995 996 997 998 999 1000 </pre>	<p>Read Infrared Sensor Values</p> <p>Map average of values to 'Cases'</p> <p>Switch to respective Case based on the location of the obstacle</p>	<pre> //Move functions for Servos void servo1_move(int _pos[2], int _steps){ for (pos = _pos[0]; pos < _pos[1]; pos += _steps){ myservo[0].write(int (pos)); delay(10); } for (pos = _pos[1]; pos > _pos[0]; pos -= _steps){ myservo[0].write(int (pos)); delay(10); } } void servo2_move(int _pos[2], int _steps){ for (pos = _pos[0]; pos < _pos[1]; pos += _steps){ myservo[1].write(int (pos)); delay(10); } for (pos = _pos[1]; pos > _pos[0]; pos -= _steps){ myservo[1].write(int (pos)); delay(10); } } </pre> <p>Based on selected case import the angle domains and send them to the servos</p>
---	---	---

Figure 16. Crease_05 Partial Arduino code.

Future application scenarios in architecture

3D mapping and surveying. One possible application is to create a swarm of *Creases* that could hypothetically self-assemble to create collective configurations or perform specific tasks. Their ability to detect and record objects in their environment and steer accordingly would enable them to avoid obstacles during navigation or conversely to surround them (Figure 19). A larger *Crease* could carry within its flat surfaces several smaller *Creases* potentially deploying on-site a swarm that involves different size elements (Figure 19). As *Crease* develops from 2D to 3D, it seems feasible to do so in real-time as other origami-based research has proven to

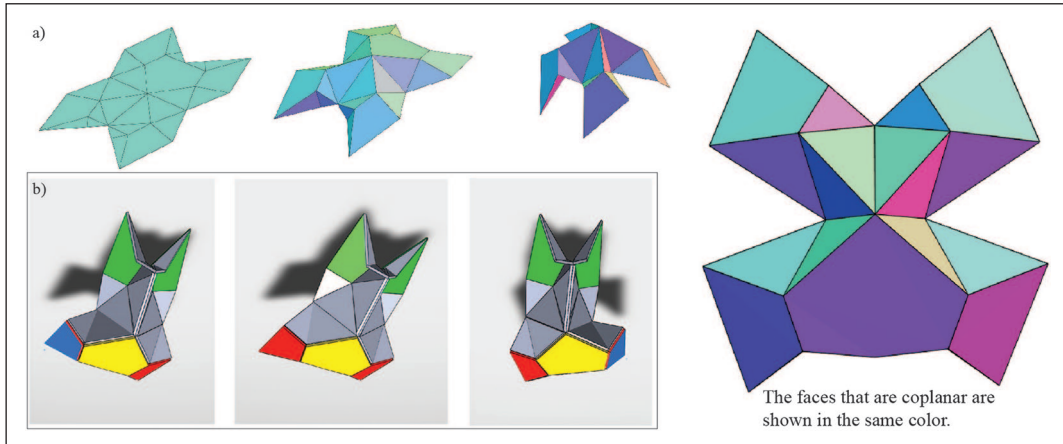


Figure 17. (a) Normal mapping where coplanar faces share the same color (b) Solidworks simulations. (Adapted from publication).³⁴

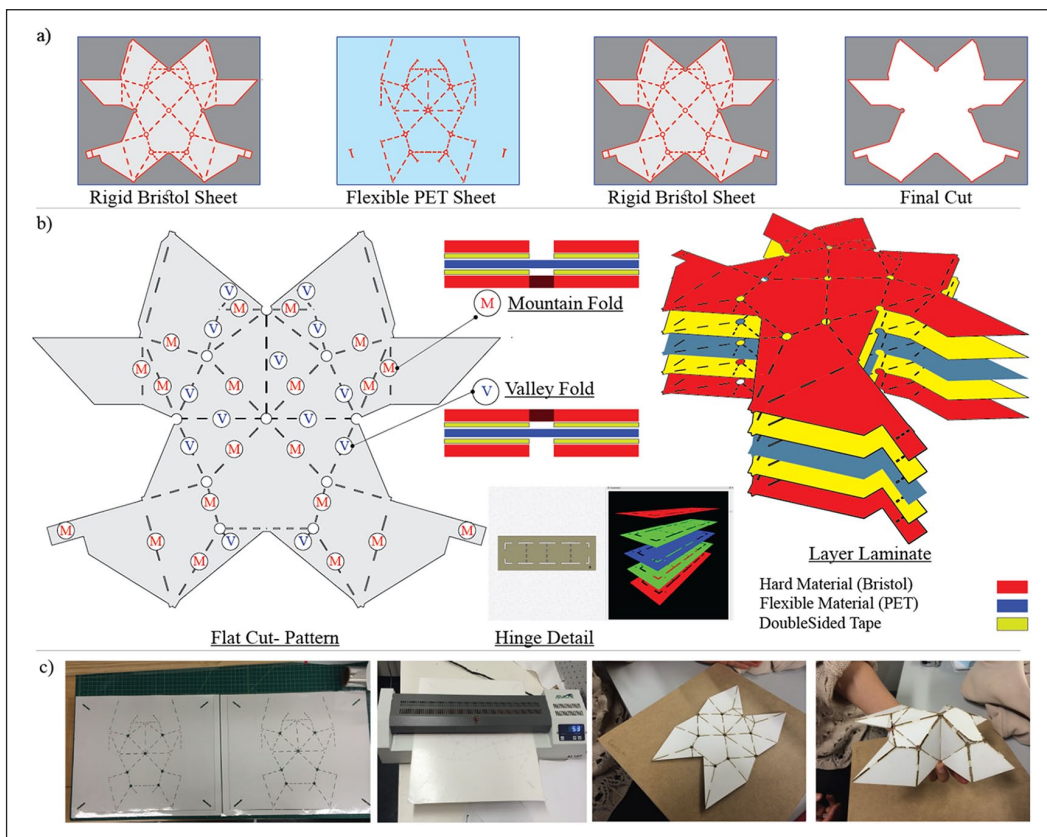


Figure 18. CAD to CAM workflow (a) Cut files generated from PopUpCAD (b) Location of valley and mountain folds on the Crease pattern and material layup (c) Fabrication steps involving material lamination, final laser-cut and prototype deployment. (Adapted from publication).³⁴



Figure 19. (a) Swarm of creases (b) Swarm surrounding object.

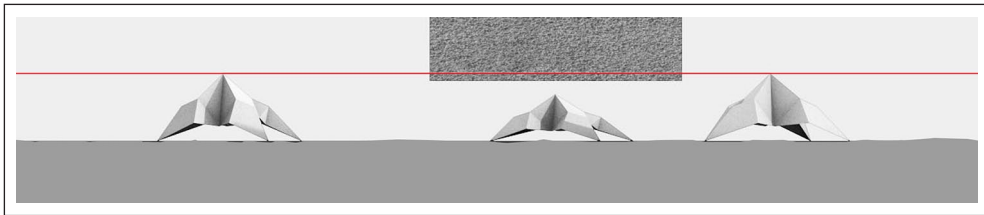


Figure 20. Obstacle navigation in the y and z-axis.

do so.⁵⁹ This would allow *Crease* to adjust its body dimensions to go underneath objects navigating difficult terrains and gaining access to areas otherwise unreachable (Figure 20). These features could be beneficial for surveying and 3D mapping architectural sites especially if these sites present challenges with accessibility.

Kinetic systems. The process of simulation, the fabrication method, and the design principles developed in the research of *Crease* hold great potential to be used in the design of kinetic architectural elements, that are flat foldable, easy to manufacture, and durable.

The geometric and kinematic principles of *Crease* allowed its interconnected planes to be activated with few motors. The kinematic chains could be applied in facades using minimal actuation. To attain this, keeping the system lightweight would be advantageous. Even though stiffness scales up exponentially with an increase in material thickness, experiments translating origami paper models to PETG have proved to be successful⁶⁰; and advances in material science, especially in polymers and thermoplastic carbon fiber composites, offer potential in producing large, light, and durable origami-based elements.⁶¹ The laminated method used in the fabrication of *Crease* could be translated into the design of kinetic architectural components. Innovations in composite lamination offer the selective programming of rigid and flexible materials within different parts of the single monolithic laminate at an architectural scale.

Crease displayed movement in response to sensing. A wide variety of smart sheet materials can be embedded within similar laminate constructions to provide added functionality like sensing⁶² to façade components. Similar methods of simulating and optimization of origami structures like *Crease* could be applied to kinetic architecture to minimize input motion and maximize output motion.

Conclusion

Responding to the objectives set at the beginning of the research, we engaged in a collaboration between the fields of design and engineering by proposing an approach that uses both quantitative and qualitative data to inform the design of our robot. The complexity in the degrees of freedom and the need for minimal actuation make it unlikely that *Crease* would have been generated solely from a traditional engineering approach without being informed by design sensibility. The design of *Crease's* geometric pattern revealed the potential to efficiently leverage folded hinges for locomotion. And the geometric pattern was refined and optimized for its input/output movement through computational means. In addition, the simple fabrication method allowed for quick trial and error iterations to arrive at solutions that would otherwise have been too computationally intensive and time-consuming. In this way, the research methods integrated physical and intuitive processes with digital workflows and simulations rather than just applying intensive computational analysis. The combination of physical prototyping and application of software used in architectural design and engineering disciplines proved to be an efficient approach to arrive at novel, refined, and optimized prototypes.

In reference to our second objective, the research presented here confirms the relationship between origami principles and kinematics producing as a result, the design of an ambulatory robot that features controlled and efficient locomotion with minimal mechanical actuation. *Crease*, the origami robot, transforms from a two-dimensional stage to a three-dimensional configuration. In the pattern of *Crease*, principles of spherical and parallel linkages were applied to amplify rotational motion throughout its body; thus, achieving an efficient yet graceful gait. As discussed through the prototypes, the relationship between the folded pattern and the type and number of actuators affects the gait and ability to steer. Sensing of obstacles for navigation control is attained through simple programming. The under-actuated nature of the robot and the employed pop-up laminate fabrication method enable the production of fast, economical, and lightweight prototyping of this robot.

In addition, the research aimed to expand robotic design to a wider audience and by doing so explore potential contributions. To support this, the method of fabrication had to be easily accessible and economical. Employing the simple fabricating technique of laminate construction and readily available flat sheets and minimal joinery enabled designers to engage in an iterative process of design producing a light-weight, easy-to-assemble ambulatory robot. Using a combination of rigid planes and a PET flexible membrane for the folds, the materials used in *Crease* are economical and readily available making the process of fabrication inexpensive. These features can be translatable beyond robotics to applications to other fields.

As explained above, our approach and solution demonstrate the applicability of architectural design thinking across disciplines. However, scale and translation are dependent on context and applications. Existing research in the translation of origami-based concepts shows promise in scaling and adapting our research to architectural applications. Elegant motion, lightness, robustness, ease in manufacturability, durability, and efficiency are critical requirements for the design of both robotics and kinetic architecture. Through this work, connections between *Crease* and kinetic elements in architecture are established by exploring architectural application scenarios. Variations of *Crease* with capabilities of sensing and recording their surroundings provide possibilities for swarms to 3D map and survey architectural sites. Whereas other features of *Crease* such as design and fabrication processes, laminate construction, hinged details, use complementary materials, etc., can be applied to the design of kinetic architectural components.

This investigation contributes both to the field of robotics and architectural design in the Age of the Fourth Industrial Revolution where tools, process, and approaches permeate back and forth from various disciplines to attain cohesive and meaningful solutions.

Acknowledgements

Authors Olga Mesa and Saurabh Mhatre contributed equally to this research, design, and analysis. Research, design, and fabrication of first *Creases* were done by Olga Mesa, Saurabh Mhatre, and Malika Singh. The authors wish to credit that

the beginning of this research was developed during a course titled: *SCI 6478 Informal Robotics / New Paradigms for Design & Construction* designed and taught by Chuck Hoberman in collaboration with Dan Aukes and Jonathan Grinham at the Harvard Graduate School of Design.

Declaration of conflicting interests

The author(s) declared no potential conflicts of interest with respect to the research, authorship, and/or publication of this article.

Funding

The author(s) received no financial support for the research, authorship, and/or publication of this article.

ORCID iD

Saurabh Mhatre  <https://orcid.org/0000-0002-7502-8302>

References

1. Perlmutter M and Breit S. The future of the MEMS inertial sensor performance, design and manufacturing. In: *2016 DGON inertial sensors and systems (ISS)*, Karlsruhe, Germany, 2016, pp. 1–12.
2. Petrš J, Dahy H and Florián M. From MoleMOD to MoleSTRING design of self-assembly structures actuated by shareable soft robots. In: *Proceedings of 37 eCAADe and XXIII SIGraDi joint conference, "Architecture in the Age of the 4th Industrial Revolution"* (eds Sousa JP, Henriques GC and Xavier JP), Porto, 2019, Blucher.
3. Felton S, Tolley M, Demaine E, et al. Applied origami. A method for building self-folding machines. *Science* 2014; 345: 644–644.
4. Aukes DM, Goldberg B, Cutkosky MR, et al. An analytic framework for developing inherently-manufacturable pop-up laminate devices. *Smart Materials and Structures* 2014; 23: 94013–94013.
5. Bowen LA, Grames CL, Magleby SP, et al. A classification of action origami as systems of spherical mechanisms. *J Mech Design* 2013; 135(11): 7.
6. Rus D and Tolley MT. Design, fabrication and control of soft robots. *Nature* 2015; 521: 467–475.
7. Vogel S. Better bent than broken. *Discover* May 1995, pp. 62–67.
8. Pister KSJ, Judy MW, Burgett SR, et al. Microfabricated hinges. *Sens Actuators A Phys* 1992; 33: 249–256.
9. Wood RJ, Avadhanula S, Sahai R, et al. Microrobot design using fiber reinforced composites. *J Mech Design* 2008; 130: 052304.
10. Sahai R, Galloway KC and Wood RJ. Elastic element integration for improved flapping-wing micro air vehicle performance. *IEEE Trans Robot* 2013; 29(1): 32–41.
11. Sharifzadeh M, Khodambashi R and Aukes DM. An integrated design and simulation environment for rapid prototyping of laminate robotic mechanisms. In: *Proceedings of the ASME design engineering technical conference*, Quebec, Canada, 26–29 August 2018, ASME.
12. Wood RJ, Avadhanula S, Menon M, et al. Microrobotics using composite materials: the micromechanical flying insect thorax. In: *International conference on robotics and automation*, Taipei, Taiwan, 2003, pp. 1842–1849. IEEE.
13. Sreetharan PS, Whitney JP, Strauss MD, et al. Monolithic fabrication of millimeter-scale machines. *J Microeng Microeng* 2012; 22(5): 55027–55027.
14. Birkmeyer P, Peterson K and Fearing RS. DASH: a dynamic 16g hexapedal robot. In: *2009 IEEE/RSJ international conference on intelligent robots and systems*, St. Louis, MO, 10–15 October 2009, pp. 2683–2689. IEEE.
15. Cybulski JS, Clements J and Prakash M. Foldscope: origami-based paper microscope. *PLoS ONE* 2014; 9(6): e98781–e98781.
16. Niiyama R, Sun X, Yao L, et al. Sticky actuator: free-form planar actuators for animated objects. In: *Proceedings of the ninth international conference on tangible, embedded, and embodied interaction*. New York, NY, 2015, pp.77–84. ACM.
17. Shigemune H, Maeda S, Hara Y, et al. Kirigami robot: Making paper robot using desktop cutting plotter and inkjet printer. In: *2015 IEEE/RSJ international conference on intelligent robots and systems (IROS) 2015*, pp. 1091–1096, IEEE, Hamburg, Germany.

18. Birglen L, Lalibert T and Gosselin CM. *Underactuated robotic hands*. 1st ed. Berlin Heidelberg: Springer Publishing Company, Incorporated, 2008.
19. Aukes D, Kim S, Garcia P, et al. Selectively compliant underactuated hand for mobile manipulation. In: *Proceedings - IEEE international conference on robotics and automation*, 2012, pp. 2824–2829, IEEE, Saint Paul, MN.
20. Firouzeh A, Salerno M and Paik J. Stiffness control with shape memory polymer in underactuated robotic origamis. *IEEE Trans Robot* 2017; 33: 765–777.
21. Raibert MH, Brown HB and Chepponis M. Experiments in balance with a 3D one-legged hopping machine. *Int J Robot Res* 1984; 3(2): 75–92.
22. Waldron K and McGhee R. Configuration design of the adaptive suspension vehicle. *IEEE Control Syst Mag* 1986; 6: 7–12.
23. Playter R, Buehler M and Raibert M. BigDog. In: *SPIE 6230, unmanned systems technology VIII, 62302O* Orlando (Kissimmee), FL, May 2006, p.6.
24. Nelson G, Saunders A, Neville N, et al. PETMAN: a humanoid robot for testing chemical protective clothing. *J of the Robot Soc Japan* 2012; 30: 372–377.
25. Robinson DW, Pratt JE, Paluska DJ, et al. Series elastic actuator development for a biomimetic walking robot. In: *IEEE/ASME international conference on advanced intelligent mechatronics* Atlanta, GA, 19–23 September 1999, pp. 561–568, IEEE.
26. Altendorfer R, Moore N, Komsuoglu H, et al. RHex: a biologically inspired hexapod runner. *Auton Robots* 2001; 11: 207–213.
27. Khoramshahi M, Spröwitz A, Tuleu A, et al. Benefits of an active spine supported bounding locomotion with a small compliant quadruped robot. In: *2013 IEEE international conference on robotics and automation*, Karlsruhe, Germany, 6–10 May 2013, pp. 3329–3334.
28. Spröwitz A, Tuleu A, Vespignani M, et al. Towards dynamic trot gait locomotion: design, control, and experiments with Cheetah-cub, a compliant quadruped robot. *Int J Rob Res* 2013; 32: 932–950.
29. Hoover AM, Steltz E and Fearing RS. RoACH: an autonomous 2.4g crawling hexapod robot. In: *2008 IEEE/RSJ international conference on intelligent robots and systems*, Nice, France, 22–26 September 2008, pp. 26–33. IEEE.
30. Haldane D, Casarez CS, Karras J, et al. Integrated manufacture of exoskeletons and sensing structures for folded millirobots. *J Mech Rob* 2015; 7(2): 19.
31. Mulgaonkar Y, Araki B, Koh J, et al. The flying monkey: a mesoscale robot that can run, fly, and grasp. In: *2016 IEEE international conference on robotics and automation (ICRA)*, Stockholm, Sweden, 2016, pp.4672–4679.
32. Jung G-P, Choi H-C and Cho K-J. The effect of leg compliance in multi-directional jumping of a flea-inspired mechanism. *Bioinspir Biomim* 2017; 12: 26006–26006.
33. Karpelson M, Wei G-Y and Wood RJ. A review of actuation and power electronics options for flapping-wing robotic insects. In: *IEEE international conference on robotics and automation* Pasadena, CA, 2008, pp.779–786, IEEE.
34. Mesa O, Mhatre S, Singh M, et al. CREASE synchronized gait through folded geometry. In: *Proceedings of 37 eCAADe and XXIII SIGraDi Joint Conference, "Architecture in the Age of the 4Th Industrial Revolution* (ed José Pedro; Henriques GCX, João Pedro), Porto, 2020, pp. 197–206. Blucher Design Proceedings.
35. Niiyama R, Rus D and Kim S. Pouch Motors: Printable/inflatable soft actuators for robotics. In: *2014 IEEE international conference on robotics and automation (ICRA)*, Hong Kong, China, 2014, pp. 6332–6337.
36. Sitti M. Piezoelectrically actuated four-bar mechanism with two flexible links for micromechanical flying insect thorax. *IEEE/ASME Trans Mechatron* 2003; 8: 26–36. DOI: 10.1109/TMECH.2003.809126.
37. Aukes DM and Wood RJ. Algorithms for Rapid Development of Inherently-Manufacturable Laminate Devices. In: *ASME 2014 conference on smart materials, adaptive structures and intelligent systems*, Newport, Rhode Island, 2014, pp.V001T001A005–V001T001A005. ASME.
38. Schenk M and Guest SD. Origami folding: a structural engineering approach. In: *5 OSME* Singapore, 2011.
39. Doshi N, Goldberg B, Sahai R, et al. Model driven design for flexure-based Microrobots. In: *2015 IEEE/RSJ international conference on intelligent robots and systems (IROS)*, Hamburg, Germany, 2015, pp. 4119–4126. IEEE.
40. Mehta A, Delpreto J and Rus D. Integrated codesign of printable robots. *J Mech Robot* 2015; 7: 021015.
41. Hammond FL, Weisz J, De La Llera Kurth AA, et al. Towards a design optimization method for reducing the mechanical complexity of underactuated robotic hands. In: *Proceedings - IEEE international conference on robotics and automation*, Minnesota, MN, 2012, pp. 2843–2850. Piscataway, NJ: IEEE.

42. Fei LJ and Sujan D. Origami theory and its applications: a literature review. *World Acad Sci Eng Techn* 2013; 229–233.
43. Macri S. *Practical application of rigid thick origami in kinetic architecture*. Manoa: University of Hawaii, 2015.
44. Nishiyama Y. Miura folding: applying origami to space exploration. *Int J Pure Appl Math* 2012; 79(2): 269–279.
45. Chen Y, Peng R and You Z. Origami of thick panels. *Science* 2015; 349(6246): 396–400.
46. Morgan MR, Lang RJ, Magleby SP, et al. Towards developing product applications of thick origami using the offset panel technique. *Mech Sci* 2016; 7: 69–77.
47. Tachi T. Rigid-foldable thick origami. In: *Origami 5: Fifth international meeting of origami science, mathematics, and education*, Singapore Management University, Singapore, 2016, pp. 253–263.
48. Turco ML, Zich U, Astolfi A, et al. From digital design to physical model: Origami techniques applied to dynamic paneling shapes for acoustic performance control. In: *35th Annual international conference eCAADe – educational and research in computer aided architectural design in Europe*, Rome, 2017 2017, pp.77–86.
49. Capone M, Lanzara E, Marsillo L, et al. Responsive complex surfaces manufacturing using origami. In: *37 education and research in computer aided architectural design in Europe and XXIII Iberoamerican society of digital graphics, joint conference (N 1)*, Porto, 2019, pp. 715–724.
50. ElGhazi YS and Mahmoud AHA. Origami explorations a generative parametric technique for kinetic cellular facade to optimize daylight performance. In: *34th eCAADe conference* (ed. Hernejoja ATÖaPM), Oulu, Finland, 2016 2016, pp. 399–408.
51. Hoberman C. Olympic arch, <https://www.hoberman.com/portfolio/olympic-arch/> (2002, accessed 24 June 2020).
52. Hoberman C. *Folding structures made of thick hinged sheets*. Patent US 7,794,019 B2 US, 2006.
53. Hoberman C. 10° (TEN DEGREES), <https://www.hoberman.com/portfolio/10-ten-degrees/> (2016, accessed 24 June 2020).
54. Attia S. Evaluation of adaptive facades: the case study of Al Bahr towers in the UAE. *QScience Connect* 2018; 2017: 5339–5339.
55. Lang RJ. *Origami design secrets: Mathematical methods for an Ancient Art*. 2nd ed. New York: A K Peters/CRC Press, 2003, 2011.
56. Tachi T. Origamizing polyhedral surfaces. *IEEE Trans Vis Comput Graph* 2010; 16: 298–311.
57. Ghassaei A, Demaine E and Gershenfeld N. Fast, Interactive Origami Simulation using {GPU} Computation. In: *Proceedings of the 7th international meeting on Origami in science, mathematics and education (OSME 2018)*, Oxford, 2018, pp. 1151–1166.
58. Piker D. Kangaroo: form finding with computational physics. *Archit Design* 2013, pp. 136–137.
59. Miyashita S, Guitron S, Ludersdorfer M, et al. An untethered miniature origami robot that self-folds, walks, swims, and degrades. In: *2015 IEEE international conference on robotics and Automation (ICRA)* Seattle, WA, 2015, pp. 1490–1496. IEEE.
60. Baerlecken D, Gentry R, Swarts M, et al. Structural, deployable folds—Design and simulation of biological inspired folded structures. *Int J Archit Comput* 2014; 12: 243–262.
61. Tiliakos N. MEMS for harsh environment sensors in aerospace applications: selected case studies. In: Kraft M and White N (eds) *MEMS for automotive and aerospace applications*. Oxford: Woodhead Publishing, 2013, pp. 245–282.
62. Ozevin D. Micro-electro-mechanical-systems (MEMS) for assessing and monitoring civil infrastructures. In: Wang ML, Lynch JP and Sohn HBT (eds) *Sensor technologies for civil infrastructures*. Cambridge, UK: Woodhead Publishing, 2014, pp. 265–294.